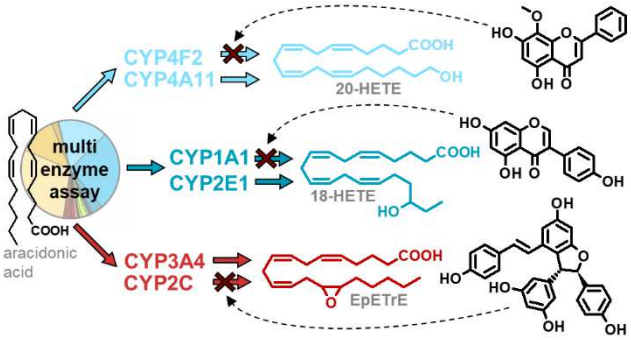

Dietary polyphenols inhibit the cytochrome P450 monooxygenase branch of the arachidonic acid cascade with remarkable structure-dependent selectivity and potency

Supporting Information

Nadja Kampschulte, Ayah Alasmer, Michael T. Empl, Michael Krohn,

Pablo Steinberg, Nils Helge Schebb

1 Oxylipin patterns of recombinant CYP and human liver and kidney microsomes

The formation of epoxy-eicosatrienoic acid (EpETrE) and hydroxy-eicosatetraenoic acid (HETE) is catalyzed by numerous CYP.[1-8] We investigated the product pattern of nine recombinant human CYP as well as human liver microsomes (HLM) and human kidney microsomes (HKM). Arachidonic acid (AA) was a substrate for all CYP enzymes used, with conversion rates ranging from 0.2 to 11 pmol min^{-1} pmol CYP^{-1} (Figure S1).

1.1 Epoxidizing CYP

The epoxidation products of AA, i.e. EpETrE (partially detected in form of their hydrolysis products DiHETrE), were the main products of epoxidizing CYP, i.e. CYP2C8, CYP2C9, CYP2C19 and CYP3A4. 19-HETE and other sub-terminal hydroxylation products were formed to different extents by the enzymes (Figure S1). Among the formed EpETrE, all four regioisomers were generated, with no epoxidation position appearing to be clearly preferred. However, the formation rates of these regioisomers differed among the enzymes. CYP2C8 formed 14(15)-EpETrE and 11(12)-EpETrE at comparable rates (1.8 and 2.1 pmol product pmol CYP^{-1} min^{-1}, respectively), while other regioisomers as well as hydroxylation products were minor side products. Similar findings were reported earlier when CYP2C8 was identified as a 14(15)-EpETrE and 11(12)-EpETrE-generating CYP enzyme[9] (52 and 48% of all EpETrE formed, respectively) and characterized with respect to the stereochemistry of the products.[10] In the case of CYP2C9, higher rates of 14(15)-EpETrE formation in comparison to 11(12)-EpETrE and especially 8(9)-EpETrE formation were reported (52, 30 and 17% for 14(15)-, 11(12)- and 8(9)-EpETrE, respectively),[9] which very well agrees with the product pattern shown herein (52% 14(15)-EpETrE, 30% 11(12)-EpETrE and 14% 8(9)-EpETrE of total EpETrE). However, in previous studies, hydroxylation products were not determined. In the present study, we show that 19-HETE is a minor product of CYP2C9-catalyzed AA oxidation and that sub-terminal hydroxylation products are formed by CYP2C8 (Figure S1). Similar product patterns were reported by Rifkind et al[4] for the AA-derived oxylipin formation in vaccinia virus-infected HepG2 cells expressing human CYP2C8 and CYP2C9. Rifkind et al.[4] also analyzed hydroxylation products and identified 18-HETE as a product of CYP2C8; however, 19- and 20-HETE were only analyzed in sum. Our results show that 19-HETE, but not 20-HETE, is a product of these CYP2C.

In line with these results on the human CYP2C subfamily, CYP2C19 primarily also gives rise to EpETrE (47% of all products formed). In addition, the 19-HETE formation rate is high (42%), while other hydroxylation products can be classified as minor side products (Figure S1), which in turn is consistent with the scientific literature.[2, 11, 12] Among the EpETrE, 11(12)-EpETrE is formed at a lower rate than the other regioisomers by CYP2C19.

About half of the marketed drugs is metabolized by CYP3A4.[13] Here we show that CYP3A4 not only leads to the formation of oxidation products of xenobiotics but also to that of lipid mediators from AA and thus may contribute to the endogenous formation of lipid mediators. CYP3A4 gave rise to epoxy-fatty acids (Figure S1), which is in good agreement with previously reported product patterns of recombinant CYP3A4.[14] Moreover, our data indicate that CYP3A4 forms a complex pattern of oxylipins, covering all aliphatic hydroxylation products as well as lipoxygenase-like mid-chain allylic hydroxy-fatty acids.[15] However, one should note that 20-HETE is not formed by CYP3A4.

1.2 ω-hydroxylating CYP

20-HETE, the product of ω-hydroxylation of AA, was formed by enzymes of the CYP4 family at remarkably high rates. In both patterns found for

CYP4A11 and CYP4F2, 20-HETE was the most present oxylipin. Other products such as EpETrE or allylic HETE were not detected in the incubations (Figure S1), which is consistent with the findings of Iamoka et al.[11] 19-HETE was formed at a lower rate in comparison to 20-HETE: It amounted to about one third of the total products of CYP4A11 and less than 10% of the total products of CYP4F2, a finding in line with results previously obtained with these CYP purified from human liver.[5]

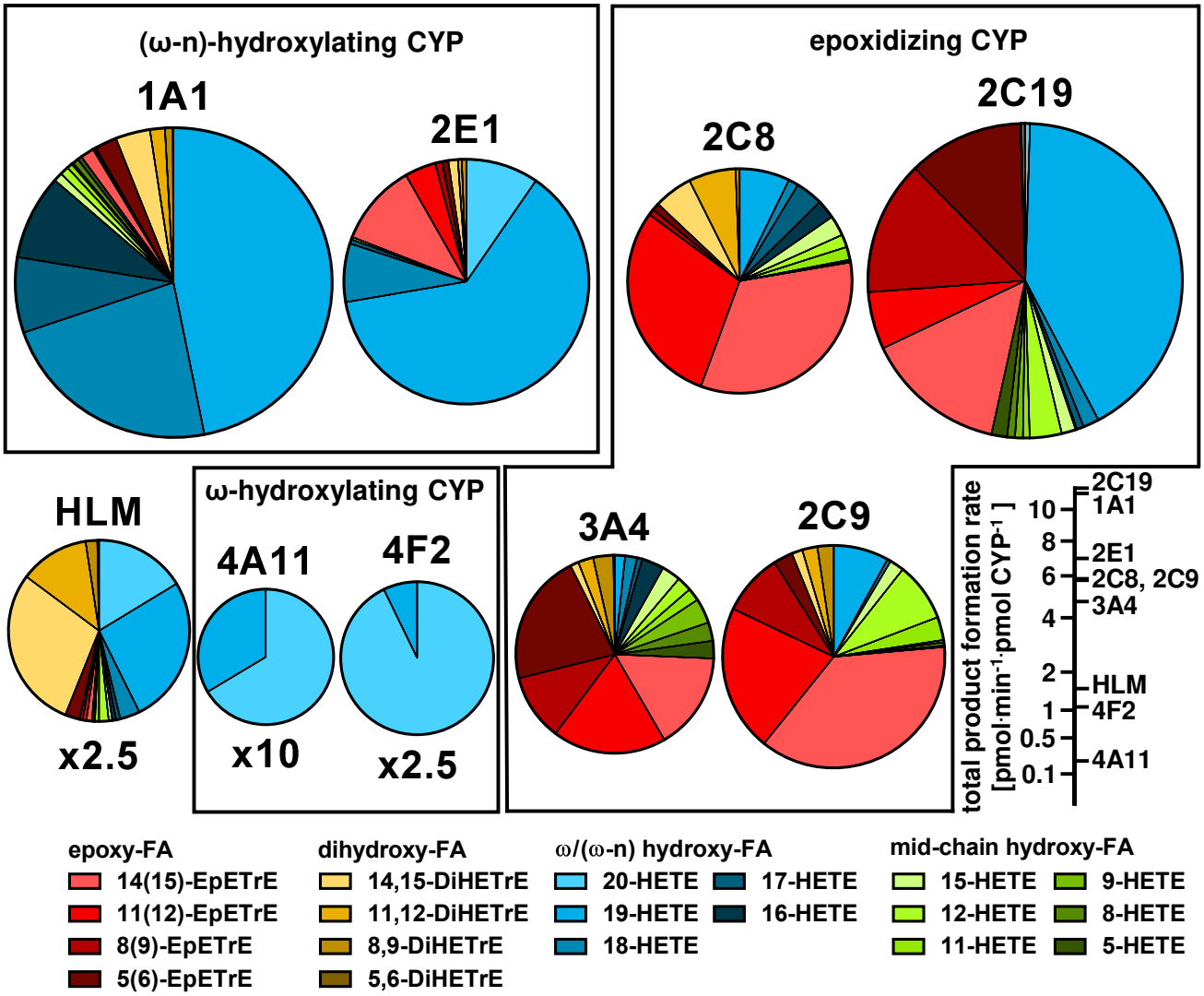

Figure S1. Product pattern of selected AA-oxidizing CYP and HLM. 100 µM AA was incubated with each CYP enzyme (25 pmol CYP mL^{-1}) or HLM (0.5 mg protein mL^{-1}; 400 pmol CYP mL^{-1}) at 37 °C for 20 min. An NADPH-generating system (1 mM NADPH) was used as co-substrate. Diagram sizes (area) represent the total product formation relative to each other (normalized to CYP content, in relation to CYP2C19 activity: 100% = 11 pmol min^{-1} pmol CYP^{-1}). Factors indicate the magnified view of the enzyme-specific diagram.

1.3 (ω-n)-Hydroxylating CYP

CYP2E1 plays a crucial role in the phase I metabolism of small, polar molecules. Our results show that this CYP enzyme also oxidizes fatty acids. 19-HETE was the main product within the group of AA-derived oxylipins formed by CYP2E1

(64% of the sum of all products formed), while 18-HETE and 20-HETE made up 8 and 9% of all products, respectively (Figure S1). Further aliphatic hydroxy-fatty acids as well as EpETrE were formed as minor side products, consistent with previously reported data on AA oxidation in CYP2E1 cDNA-transfected human HepG2 hepatoma cells (19- and 20-HETE > 90% of all metabolites).[4]

Besides CYP2E1, also CYP1A1 predominantly formed (ω-n) hydroxy-fatty acids (Figure S1). All four isomers were generated and represent 86% of all products formed. The ω-hydroxylation product 20-HETE was not formed. 19-HETE and 18-HETE made up the majority of the (ω-n)-HETE formed (47 and 22% of all products, respectively), which is consistent with findings by Falck et al.,[16] who reported the same amounts of 19-HETE (46%), 18-HETE (19%) as well as (ω-n)-HETE (87%) in the product pattern of CYP1A1 purified from rat liver.

1.4 Human liver and kidney microsomes

In incubations of AA with human liver microsomes (HLM), both EpETrE and HETE were formed. In the resulting product pattern, EpETrE (and their hydrolysis products DiHETrE) made up about 50%, while the other half were mono-hydroxylated fatty acids, mainly 19-HETE and 20-HETE (Figure 2), which is in good agreement with previous data.[4, 15, 17, 18] It should be noted that not all recent studies differentiated 20-HETE and (ω-n)-HETE, but summarized them as "terminal HETE". Among the "terminal HETE" examined here, 19-HETE was the main product in HLM; 20-HETE was formed at a slightly lower rate. 18-HETE and further (ω-n)-HETE as well as mid-chain HETE were also formed by HLM, although they only contributed to a limited extent to the overall sum of products.

All of the investigated epoxidizing enzymes, i.e. CYP2C8, CYP2C9, CYP2C19 and CYP3A4, are expressed in human liver.[19-21] Consistent with the products of these enzymes (Figure S1), 14(15)-EpETrE was the most abundant epoxy-fatty acids regioisomer in the product pattern of HLM. Most of the epoxy-fatty acids generated in HLM were detected in form of their hydrolysis products, thereby indicating that residues of soluble epoxide hydrolase (sEH) activity or other enzymes leading to the hydrolysis of the epoxide structure, for instance lipid rafts comprised by CYP and microsomal epoxide hydrolase,[22-24] were present in the microsomal preparations. 5(6)-EpETrE was found to be less hydrolyzed in comparison to the other EpETrE regioisomers. This is consistent with the regioselectivity of sEH activity: epoxide moieties close to the Δ-terminus of the fatty acids are hydrolyzed at lower rates,[25, 26] Thus, based on the product pattern, contamination with the cytosolic sEH seems to contribute to DiHETrE formation.

Consistent with the product pattern of CYP expressed in human liver, mid-chain HETE were minor products in the microsomal incubations. Among the mid-HETE, 12-HETE was formed to the highest extent in human liver microsomes, as previously reported in the scientific literature.[27, 28] Mid-chain HETE were CYP-unspecific minor products of CYP1A1, the CYP2C subfamily and CYP3A4 (Figure S1). All in all, due to low formation rates as well as unspecific regionselectivity regarding CYP-catalyzed mid-chain HETE formation, it might be assumed that they do not relevantly contribute to the endogenous 5-HETE, 12-HETE and 15-HETE formation, which are major products of lipoxygenase action.

Microsomes obtained from human kidney (HKM) also metabolize AA to oxylipins (Figure S2)). We found out that 20-HETE was the main metabolite, along with 19-HETE, while epoxy-fatty acids and their hydrolysis products were minor side products, consistent with the high expression of CYP4 in human kidney.[29-31] Due to the absence of EpETrE-forming CYP, HKM do not allow a further investigation of this pathway and are therefore not suitable for comprehensive studies on the CYP-branch of the AA cascade.

Laska et al.[6] compared CYP4 levels in HKM and HLM as well as the 20-HETE formation rate in both tissue preparations. They found that 20-HETE was formed at a four times higher rate in HLM, which can be explained by higher CYP4 levels in liver. These findings underline that HLM are the more appropriate multi-enzyme source for the investigation of CYP-catalyzed oxylipin formation when compared to HKM.

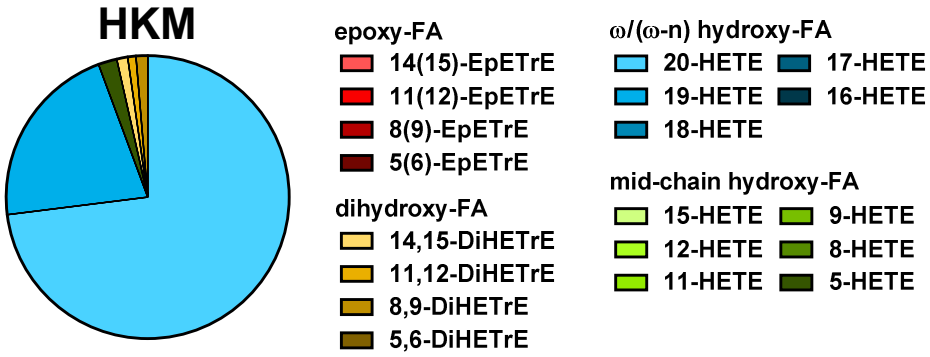

Figure S2. Pattern of oxylipins formed in human kidney microsomes (HKM). 100 µM AA was incubated with 0.5 mg HKM protein mL^{-1} and an NADPH-generating system (1 mM NADPH) as co-substrate at 37 °C for 20 min.

2 LC-MS method for the quantification of oxylipins
Liquid chromatography was performed using a 1260 LC System (Agilent, Waldbronn, Germany) composed of a binary pump and a column oven as well as a CTC-Pal autosampler (CTC analytics, Zwingen, Switzerland). Separation of the analytes (10 µL injection volume) was carried out on a Zorbax Eclipse Plus C18 reversed phase column (2.1 × 150 mm, particle size 1.8 µm; 9.5 nm pore size; Agilent) at 40 °C with a solvent flow of 300 µL min^{-1}. A SecurityGuard Ultra C18 cartridge (2.1 × 2 mm; Phenomenex, Aschaffenburg, Germany) was used as pre-column. The mobile phase consisted of 0.1% acetic acid with 5% solvent B (v/v) as solvent A and 800/150/1 (v/v/v) acetonitrile/methanol/acetic acid as solvent B. The following binary gradient was used: initial 60% B, 0.0–10.0 min linear from 60% B to 62% B, 10.0–15.0 min linear from 62% B to 98% B, 15.0–19.0 min isocratic 98% B, return to 60% B in 0.5 min and reconditioning for 1.5 min.

Table S1. Product pattern of AA oxidation by CYP and microsomes.

Formation rates [fmol product min^{-1} pmol CYP^{-1}] of oxylipins catalyzed by CYP and microsomes from human liver (HLM) as well as human kidney microsomes (HKM). 100 µM AA was incubated with each CYP enzyme (25 pmol CYP mL^{-1}) or human microsomes (0.5 mg protein mL^{-1}) at 37 °C for 20 min. An NADPH-generating system (1 mM NADPH) was applied as co-substrate. Oxylipin levels in control incubations without co-substrate were subtracted. Mean ± SD are shown, n = 3.

	2C8	2C9	2C19	4F2	4A11	2E1	1A1	3A4	HLM	HKM[1]
14,15-DiHETrE	320 ± 40	86 ± 18	8.8 ± 1	-	-	86 ± 4	380 ± 140	60 ± 2	435 ± 15	0.2 ± 0.04
11,12-DiHETrE	400 ± 40	126 ± 18	3 ± 6	-	-	34 ± 2	166 ± 50	112 ± 6	185 ± 8	0.15 ± 0.05
8,9-DiHETrE	34 ± 4	134 ± 14	38 ± 4	-	-	42 ± 2	88 ± 16	146 ± 8	31 ± 0.8	0.21 ± 0.08
5,6-DiHETrE	-	-	5.6 ± 0.2	-	-	-	8 ± 2	10.6 ± 0.4	4.3 ± 0.3	-
14(15)-EpETrE	1520 ± 160	2200 ± 400	1660 ± 180	-	-	740 ± 60	152 ± 14	700 ± 80	14 ± 1	-
11(12)-EpETrE	1700 ± 100	1200 ± 200	680 ± 60	-	-	306 ± 16	24 ± 4	840 ± 80	10.3 ± 0.3	-
8(9)-EpETrE	50 ± 4	500 ± 120	1580 ± 140	-	-	62 ± 6	12.6 ± 1.8	480 ± 40	8.25 ± 0.5	-
5(6)-EpETrE	62 ± 2	160 ± 20	1360 ± 60	-	-	56 ± 6	240 ± 20	960 ± 20	40 ± 5	-
20-HETE	-	-	58 ± 6	1000 ± 200	140 ± 30	660 ± 40	-	-	243 ± 15	11.9 ± 0.8
19-HETE	420 ± 60	460 ± 20	4800 ± 200	80 ± 20	72 ± 4	4600 ± 600	5000 ± 200	74 ± 8	400 ± 25	3.5 ± 1
18-HETE	20 ± 20	30 ± 6	186 ± 4	-	-	540 ± 60	2400 ± 140	88 ± 4	52.5 ± 2.5	-
17-HETE	220 ± 20	-	84 ± 2	-	-	40 ± 4	860 ± 60	36 ± 4	11 ± 2	-
16-HETE	158 ± 6	-	13 ± 1.6	-	-	-	960 ± 80	164 ± 12	10.3 ± 0.8	-
15-HETE	160 ± 20	116 ± 14	168 ± 6	-	-	-	100 ± 14	136 ± 8	9.5 ± 1.5	-
12-HETE	106 ± 12	480 ± 40	376 ± 14	-	-	-	98 ± 6	106 ± 2	3.8 ± 0.5	-
11-HETE	112 ± 16	190 ± 16	80 ± 4	-	-	22 ± 2	62 ± 8	94 ± 6	25.8 ± 1.8	-
9-HETE	-	16 ± 4	92 ± 10	-	-	-	22 ± 2	180 ± 12	2.3 ± 0.8	-
8-HETE	16 ± 6	26 ± 8	92 ± 6	-	-	-	66 ± 10	134 ± 8	11 ± 0.5	-
5-HETE	5.4 ± 0.4	14 ± 2	182 ± 18	-	-	-	46 ± 4	128 ± 2	2 ± 0.3	0.34 ± 0.07

[1][pmol product min^{-1} mg $protein^{-1}$]

Table S2. MS parameters for the quantification of oxylipins formed in microsomal incubations

	name	Q1	Q3	retention time [min]	DP [V]	CE [V]	internal standard	calibration range LLOQ[1] [nM]	calibration range ULOQ[2] [nM]
analytes	14,15-DiHETrE	337.2	207.1	7.87	-30	-25	d11-11(12)-DiHETrE	4.7	2350
	11,12-DiHETrE	337.2	167.1	9.02	-40	-27	d11-11(12)-DiHETrE	7.5	7500
	8,9-DiHETrE	337.2	127.1	10.06	-35	-26	d11-11(12)-DiHETrE	4.7	4650
	5,6-DiHETrE	337.2	145.1	11.70	-35	-26	d11-11(12)-DiHETrE	9.4	2350
	19-HETE	319.2	275.1	11.17	-55	-23	d8-15-HETE	100	1000
	20-HETE	319.2	275.1	11.61	-60	-23	d8-15-HETE	250	1000
	18-HETE	319.2	261.0	12.44	-50	-23	d8-15-HETE	25	1000
	17-HETE	319.2	247.0	12.72	-50	-23	d8-15-HETE	25	1000
	16-HETE	319.2	233.0	12.90	-50	-23	d8-15-HETE	50	1000
	15-HETE	319.2	219.2	13.91	-50	-25	d8-15-HETE	44	440
	11-HETE	319.2	167.2	14.28	-45	-23	d8-12-HETE	4.4	440
	8-HETE	319.2	155.2	14.51	-45	-22	d8-12-HETE	24	940
	12-HETE	319.2	179.2	14.53	-45	-23	d8-12-HETE	10	1000
	9-HETE	319.2	167.2	14.27	-40	-20	d8-5-HETE	27	530
	5-HETE	319.2	115.2	14.89	-45	-20	d8-5-HETE	7.0	700
	14(15)-EpETrE	319.2	219.3	15.35	-30	-24	d11-14(15)-EpETrE	39	1950
	11(12)-EpETrE	319.3	167.2	15.66	-30	-24	d11-14(15)-EpETrE	13	1250
	8(9)-EpETrE	319.2	155.2	15.76	-35	-20	d11-14(15)-EpETrE	70	700
	5(6)-EpETrE	319.2	191.1	15.87	-35	-20	d11-14(15)-EpETrE	125	1250
internal standards	d11-11(12)-DiHETrE	348.2	167.1	8.78	-40	-27			
	d8-15-HETE	327.0	226.0	13.77	-35	-20			
	d8-12-HETE	327.2	184.2	14.42	-45	-23			
	d8-5-HETE	327.2	116.1	14.80	-45	-20			
	d11-14(15)-EpETrE	330.2	219.3	15.28	-30	-24			

[1]LLOQ was set to the lowest calibration standard yielding a signal to noise ratio ≥ 5 and an accuracy within the calibration curve of ± 20 %.
[2]ULOQ concentration does not represent the end of the linear range, but is the highest calibration standard injected
MS source settings: ion spray voltage: -4500 V, curtain gas (N_2): 20 psi, nebulizer gas (gas 1, zero air): 70 psi, drying gas (gas 2, zero air): 55 psi, temperature 500 °C

3 Fluorescence assay

The 7-methoxy-4-trifluoro-methylcoumarin (MFC)-based CYP2C assay was carried out in a 96-well micro titer plate in 0.1 M potassium phosphate buffer (pH 7.4) in a final volume of 200 µL. CYP2C9 (25 pmol CYP/mL) was preincubated with MFC (8 µM) and sulfaphenazole or hopeaphenol for 10 min at 37 °C. The reactions were started by the addition of an NADPH-generating system (final concentration: 1 mM NADPH, 1 U mL^{-1} glucose-6-phophate-dehydrogenase, 3.8 mM glucose-6-phosphate, 4.3 mM magnesium chloride). After 60 min incubation at 37 °C, the fluorescence of the MFC metabolite was measured at excitation and emission wavelengths of 535 and 405 nm, respectively.

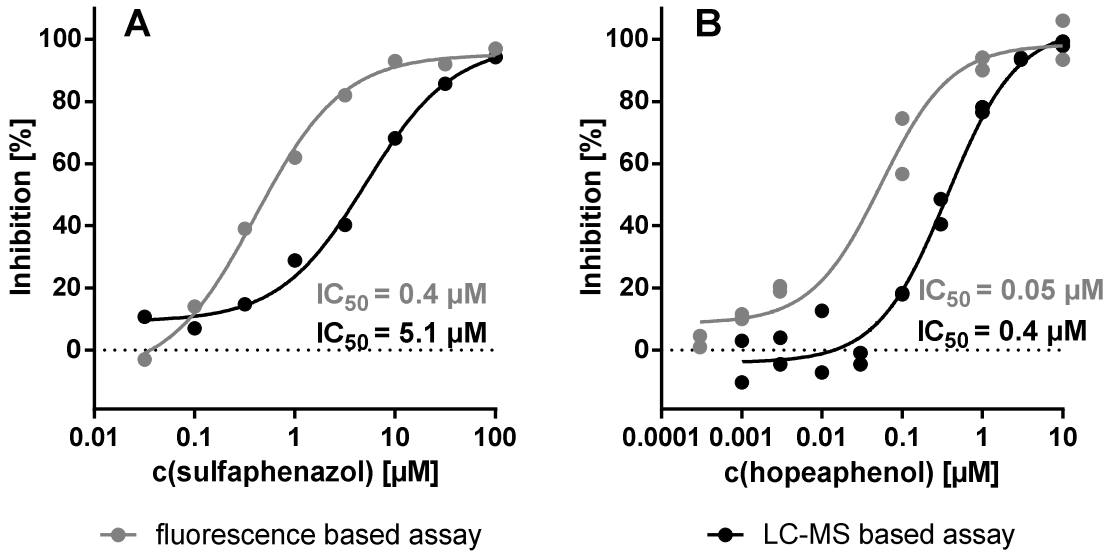

Figure S3. Comparison of IC_{50} values of (A) the CYP inhibitor sulfaphenazole and (B) the polyphenol hopeaphenol in two different assays. In the LC-MS-based assay, the inhibition of CYP2C9-catalyzed EpETrE formation from AA was measured by determination of EpETrE by means of LC-MS. In the fluorescence-based assay, the fluorophore HFC, an MFC metabolite, was measured in order to evaluate CYP2C9 inhibition. Inhibition was calculated based on product formation relative to control incubations. IC_{50} values were calculated by fitting the data to a sigmoidal concentration-response curve.

4 Metabolism of polyphenols

To investigate the metabolism of polyphenols in human liver microsomes during the incubation of the fatty acid, each polyphenol (100 µM) was incubated as described in the absence of AA. After the termination of the reaction, flavone (2.5 nmol) was added as internal standard. Following liquid/liquid extraction with ethyl acetate, evaporation of the solvent and reconstitution in methanol, the extract was analyzed by means of LC-UV. The determination of polyphenols was carried out on a Merck-Hitachi HPLC system (interface L-7000, quaternary pump L-7100, autosampler L-7250, photodiode array (PDA) detector L-7455). Chromatographic separation (10 µL injection volume) was carried out on an RP18-phase (100 × 3.0 mm, 2.6 µm core shell particles, 10 nm pore size) with the following binary gradient of water and acetonitrile (flow rate: 0.5 mL min^{-1}) at 55 °C: 0.0–10.0 min isocratic 5% acetonitrile, 10.0–60.0 min linear from 5% to 40% acetonitrile, from 60.0–60.50 min linear to 100%

acetonitrile, isocratic 100% acetonitrile for 6.5 min, then returning to initial conditions in 0.5 min, followed by reconditioning for 7.5 min. The polyphenols were detected by a PDA detector operated with a slit of 4 nm and a frequency of 5 Hz in the range of 220–320 nm. The absorption maximum of each polyphenol was used in order to evaluate the respective chromatogram (Table S3).

Table S3. Recovery of polyphenols after incubation with human liver microsomes[a].

	λ [nm][b]	**recovery [%][c]**
apigenin	265	> 95%
nobiletin	248	90%
wogonin	274	> 95%
genistein	258	> 95%
ε-viniferin	319	> 95%
hopeaphenol	220	> 95%

[a]:Each polyphenol (100 µM) was incubated with 0.5 mg HLM protein mL^{-1} for 20 min with an NADPH-generating system

[b]Absorption maximum of the respective compound and wavelength at which the respective chromatograms were evaluated

[c]Relative to control incubations without NADPH

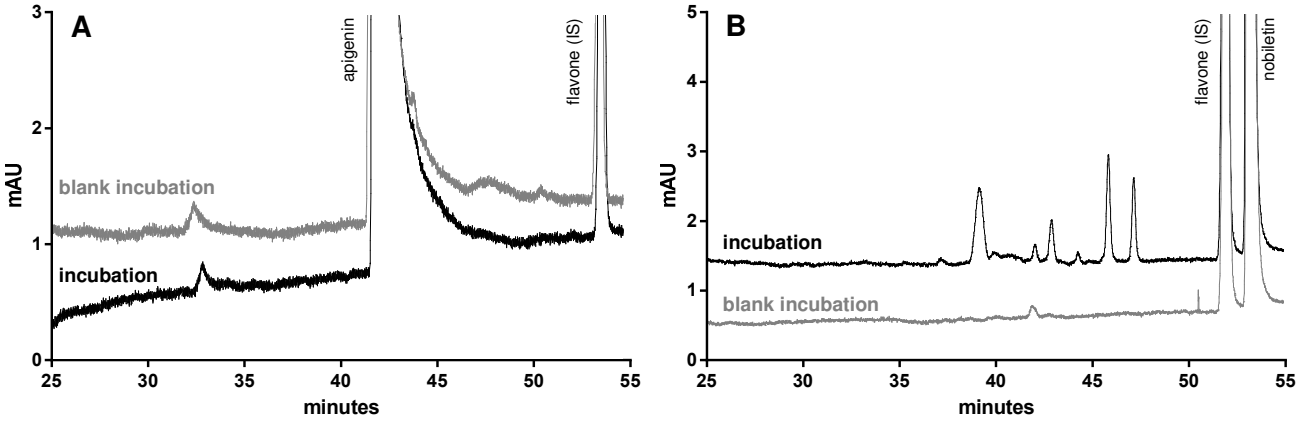

Figure S4. Recovery and metabolites of (A) apigenin and (B) nobiletin after incubation with human liver microsomes (HLM). The polyphenol (100 µM) was incubated with HLM (0.5 mg protein ml^{-1}) for 20 min. at 37 °C with and without (blank) an NADPH-generating system (1 mM NADPH, 1 U mL^{-1} glucose-6-phophate-dehydrogenase, 3.8 mM glucose-6-phosphate, 4.3 mM $MgCl_2$).

Under the present experimental conditions, the recovery of the polyphenols after the incubation was > 95%. Furthermore, no metabolites were detected in the LC-UV chromatogram (Figure S4A, Table S3) with one exception: Only about 90% of nobiletin were recovered after incubation with HLM. At the same time, additional peaks were detected in the LC-UV chromatogram (Figure S4B). Based on retention time and absorption spectrum, it can be assumed that these were nobiletin metabolites. Thus, the inhibition of CYP1A1 by nobiletin is probably due to the metabolism of this polyphenol by CYP1A1.[32] One can conclude that under the given conditions no significant turnover of the other polyphenols occurred.

Oxylipin formation and inhibition in HCT 116 cells

The CYP product pattern in HTC 116 cells was dominated by EpETrE. Only a small fraction of these oxylipins was detected as DiHETrE. The high levels of 5-HETE were probably due to 5-LOX activity in this cell line,[33] while CYP only contributed to a limited extent to the formation of this metabolite. 20-HETE, an oxylipin exclusively formed by CYP, was also detected in HCT 116 cells, while (ω-n)-HETE were not formed (Figure S5). EpETrE formation is consistent with the reported expression of CYP2C8, CYP2C9 and CYP2C19 in this cell line.34, 35

Hydroxy-fatty acids formation in HCT 116 cell culture supernatants as well as in supernatants derived from other cell lines following supplementation of fatty acid ethyl esters was previously reported by Ostermann et al.[36] The authors observed increased 8-HETE and 12-HETE formation, while other HETE such as 20-HETE were not detected. However, in the present study, the oxylipins were determined in the cells following sonication and saponification of lipids. Thus, one can conclude that most of the investigated lipid mediators are not secreted into the culture media.36

The formation of 20-HETE in HCT 116 cells was inhibited by the CYP inhibitor ketoconazole with an IC50 value of 5.6 µM (95% CI: 0.92–34 µM) and, thus, with same potency as in HLM. No inhibition of EpETrE formation by apigenin or ketoconazole was observed. This can be explained by the lower potency of ketoconazole regarding EpETrE formation in HLM. Furthermore, it might be possible that CYP isoenzymes such as CYP2C19 or those not under investigation in this study, which are not inhibited by ketoconazole or apigenin, contribute to EpETrE formation.

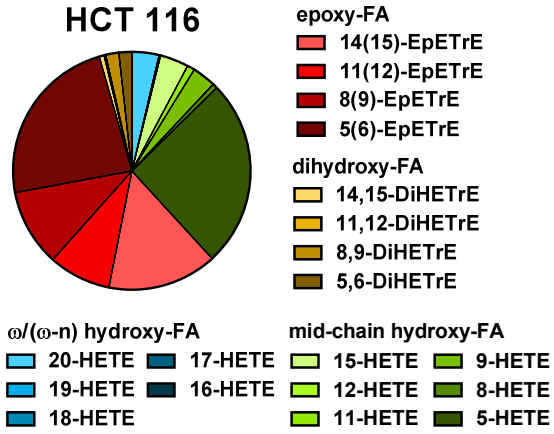

Figure S5. Pattern of oxylipins formed in HCT 116 cells. 12×10^6 cells were incubated with 10 µM AA for 24 h. Oxylipins in the cells were determined following sonication and saponification of lipids. Oxylipin levels in control incubations (without AA supplementation) were subtracted.

References:

1. Westphal, C.; Konkel, A.; Schunck, W.-H., Cytochrome P450 enzymes in the bioactivation of polyunsaturated fatty acids and their role in cardiovascular disease. In *Monooxygenase, Peroxidase and Peroxygenase Properties and Mechanisms of Cytochrome P450*, Hrycay, E. G.; Bandiera, S. M., Eds. Springer International Publishing: Cham, 2015; pp 151-187.

2. Arnold, C.; Markovic, M.; Blossey, K.; Wallukat, G.; Fischer, R.; Dechend, R.; Konkel, A.; von Schacky, C.; Luft, F. C.; Muller, D. N.; Rothe, M.; Schunck, W. H., Arachidonic acid-metabolizing cytochrome P450 enzymes are targets of {omega}-3 fatty acids. *The Journal of biological chemistry* **2010,** *285* (43), 32720-33.

3. Roman, R. J., P-450 metabolites of arachidonic acid in the control of cardiovascular function. *Physiol Rev* **2002,** *82* (1), 131-85.

4. Rifkind, A. B.; Lee, C.; Chang, T. K.; Waxman, D. J., Arachidonic acid metabolism by human cytochrome P450s 2C8, 2C9, 2E1, and 1A2: regioselective oxygenation and evidence for a role for CYP2C enzymes in arachidonic acid epoxygenation in human liver microsomes. *Arch Biochem Biophys* **1995,** *320* (2), 380-9.

5. Powell, P. K.; Wolf, I.; Jin, R.; Lasker, J. M., Metabolism of arachidonic acid to 20-hydroxy-5,8,11, 14-eicosatetraenoic acid by P450 enzymes in human liver: involvement of CYP4F2 and CYP4A11. *J Pharmacol Exp Ther* **1998,** *285* (3), 1327-36.

6. Lasker, J. M.; Chen, W. B.; Wolf, I.; Bloswick, B. P.; Wilson, P. D.; Powell, P. K., Formation of 20-hydroxyeicosatetraenoic acid, a vasoactive and natriuretic eicosanoid, in human kidney. Role of Cyp4F2 and Cyp4A11. *The Journal of biological chemistry* **2000,** *275* (6), 4118-26.

7. Zeldin, D. C., Epoxygenase pathways of arachidonic acid metabolism. *The Journal of biological chemistry* **2001,** *276* (39), 36059-62.

8. Wu, S.; Moomaw, C. R.; Tomer, K. B.; Falck, J. R.; Zeldin, D. C., Molecular cloning and expression of CYP2J2, a human cytochrome P450 arachidonic acid epoxygenase highly expressed in heart. *The Journal of biological chemistry* **1996,** *271* (7), 3460-8.

9. Zeldin, D. C.; DuBois, R. N.; Falck, J. R.; Capdevila, J. H., Molecular cloning, expression and characterization of an endogenous human cytochrome P450 arachidonic acid epoxygenase isoform. *Arch Biochem Biophys* **1995,** *322* (1), 76-86.

10. Daikh, B. E.; Lasker, J. M.; Raucy, J. L.; Koop, D. R., Regio- and stereoselective epoxidation of arachidonic acid by human cytochromes P450 2C8 and 2C9. *J Pharmacol Exp Ther* **1994,** *271* (3), 1427-33.

11. Imaoka, S.; Hashizume, T.; Funae, Y., Localization of rat cytochrome P450 in various tissues and comparison of arachidonic acid metabolism by rat P450 with that by human P450 orthologs. *Drug Metab Pharmacok* **2005,** *20* (6), 478-84.

12. Fer, M.; Dreano, Y.; Lucas, D.; Corcos, L.; Salaun, J. P.; Berthou, F.; Amet, Y., Metabolism of eicosapentaenoic and docosahexaenoic acids by recombinant human cytochromes P450. *Arch Biochem Biophys* **2008,** *471* (2), 116-25.

13. Guengerich, F. P., Cytochrome p450 and chemical toxicology. *Chem Res Toxicol* **2008,** *21* (1), 70-83.

14. Lucas, D.; Goulitquer, S.; Marienhagen, J.; Fer, M.; Dreano, Y.; Schwaneberg, U.; Amet, Y.; Corcos, L., Stereoselective epoxidation of the last double bond of polyunsaturated fatty acids by human cytochromes P450. *J Lipid Res* **2010,** *51* (5), 1125-33.

15. Bylund, J.; Kunz, T.; Valmsen, K.; Oliw, E. H., Cytochromes P450 with bisallylic hydroxylation activity on arachidonic and linoleic acids studied with human recombinant enzymes and with human and rat liver microsomes. *J Pharmacol Exp Ther* **1998,** *284* (1), 51-60.

16. Falck, J. R.; Lumin, S.; Blair, I.; Dishman, E.; Martin, M. V.; Waxman, D. J.;

Guengerich, F. P.; Capdevila, J. H., Cytochrome P-450-dependent oxidation of arachidonic acid to 16-, 17-, and 18-hydroxyeicosatetraenoic acids. *The Journal of biological chemistry* **1990,** *265* (18), 10244-9.

17. Zeldin, D. C.; Moomaw, C. R.; Jesse, N.; Tomer, K. B.; Beetham, J.; Hammock, B. D.; Wu, S., Biochemical characterization of the human liver cytochrome P450 arachidonic acid epoxygenase pathway. *Arch Biochem Biophys* **1996,** *330* (1), 87-96.

18. Rifkind, A. B., CYP1A in TCDD toxicity and in physiology-with particular reference to CYP dependent arachidonic acid metabolism and other endogenous substrates. *Drug Metab Rev* **2006,** *38* (1-2), 291-335.

19. Song, W.; Yu, L.; Peng, Z., Targeted label-free approach for quantification of epoxide hydrolase and glutathione transferases in microsomes. *Anal Biochem* **2015,** *478*, 8-13.

20. Michaels, S.; Wang, M. Z., The revised human liver cytochrome P450 "Pie": absolute protein quantification of CYP4F and CYP3A enzymes using targeted quantitative proteomics. *Drug Metab Dispos* **2014,** *42* (8), 1241-51.

21. Ohtsuki, S.; Schaefer, O.; Kawakami, H.; Inoue, T.; Liehner, S.; Saito, A.; Ishiguro, N.; Kishimoto, W.; Ludwig-Schwellinger, E.; Ebner, T.; Terasaki, T., Simultaneous absolute protein quantification of transporters, cytochromes P450, and UDP-glucuronosyltransferases as a novel approach for the characterization of individual human liver: comparison with mRNA levels and activities. *Drug Metab Dispos* **2012,** *40* (1), 83-92.

22. Orjuela Leon, A. C.; Marwosky, A.; Arand, M., Evidence for a complex formation between CYP2J5 and mEH in living cells by FRET analysis of membrane protein interaction in the endoplasmic reticulum (FAMPIR). *Arch Toxicol* **2017,** *91* (11), 3561-3570.

23. Marowsky, A.; Meyer, I.; Erismann-Ebner, K.; Pellegrini, G.; Mule, N.; Arand, M., Beyond detoxification: a role for mouse mEH in the hepatic metabolism of endogenous lipids. *Arch Toxicol* **2017,** *91* (11), 3571-3585.

24. Marowsky, A.; Burgener, J.; Falck, J. R.; Fritschy, J. M.; Arand, M., Distribution of soluble and microsomal epoxide hydrolase in the mouse brain and its contribution to cerebral epoxyeicosatrienoic acid metabolism. *Neuroscience* **2009,** *163* (2), 646-61.

25. Zeldin, D. C.; Kobayashi, J.; Falck, J. R.; Winder, B. S.; Hammock, B. D.; Snapper, J. R.; Capdevila, J. H., Regio- and enantiofacial selectivity of epoxyeicosatrienoic acid hydration by cytosolic epoxide hydrolase. *The Journal of biological chemistry* **1993,** *268* (9), 6402-7.

26. Morisseau, C.; Hammock, B. D., Impact of soluble epoxide hydrolase and epoxyeicosanoids on human health. *Annu Rev Pharmacol* **2013,** *53*, 37-58.

27. El-Sherbeni, A. A.; El-Kadi, A. O., Repurposing resveratrol and fluconazole to modulate human cytochrome P450-mediated arachidonic acid metabolism. *Mol Pharm* **2016,** *13* (4), 1278-88.

28. Capdevila, J.; Yadagiri, P.; Manna, S.; Falck, J. R., Absolute configuration of the hydroxyeicosatetraenoic acids (HETEs) formed during catalytic oxygenation of arachidonic acid by microsomal cytochrome P-450. *Biochem Bioph Res Co* **1986,** *141* (3), 1007-11.

29. Cummings, B. S.; Lasker, J. M.; Lash, L. H., Expression of glutathione-dependent enzymes and cytochrome P450s in freshly isolated and primary cultures of proximal tubular cells from human kidney. *J Pharmacol Exp Ther* **2000,** *293* (2), 677-85.

30. Karara, A.; Dishman, E.; Jacobson, H.; Falck, J. R.; Capdevila, J. H., Arachidonic acid epoxygenase. Stereochemical analysis of the endogenous epoxyeicosatrienoic acids of human kidney cortex. *FEBS Lett* **1990,** *268* (1), 227-30.

31. Knights, K. M.; Rowland, A.; Miners, J. O., Renal drug metabolism in humans: the potential for drug-endobiotic interactions involving cytochrome P450 (CYP) and UDP-glucuronosyltransferase (UGT). *Br J Clin Pharmacol* **2013,** *76* (4), 587-602.

32. Koga, N.; Ohta, C.; Kato, Y.; Haraguchi, K.; Endo, T.; Ogawa, K.; Ohta, H.; Yano, M., In vitro metabolism of nobiletin, a polymethoxy-flavonoid, by human liver microsomes and cytochrome P450. *Xenobiotica* **2011,** *41* (11), 927-33.

33. Lepage, C.; Liagre, B.; Cook-Moreau, J.; Pinon, A.; Beneytout, J. L., Cyclooxygenase-2 and 5-lipoxygenase pathways in diosgenin-induced apoptosis in HT-29 and HCT-116 colon cancer cells. *Int J Oncol* **2010,** *36* (5), 1183-91.

34. Burns, K. E.; Shepherd, P.; Finlay, G.; Tingle, M. D.; Helsby, N. A., Indirect regulation of CYP2C19 gene expression via DNA methylation. *Xenobiotica* **2018,** *48* (8), 781-792.

35. Wang, W.; Yang, J.; Edin, M. L.; Wang, Y.; Luo, Y.; Wan, D.; Yang, H.; Song, C.-Q.; Xue, W.; Sanidad, K. Z.; Song, M.; Bisbee, H. A.; Bradbury, J. A.; Nan, G.; Zhang, J.; Shih, P.-a. B.; Lee, K. S. S.; Minter, L. M.; Kim, D.; Xiao, H.; Liu, J.-Y.; Hammock, B. D.; Zeldin, D. C.; Zhang, G., Targeted metabolomics identifies the cytochrome P450 monooxygenase eicosanoid pathway as a novel therapeutic target of colon tumorigenesis. *Cancer Res* **2019,** *79* (8), 1822.

36. Ostermann, A. I.; Willenberg, I.; Weylandt, K. H.; Schebb, N. H., Development of an online-SPE–LC–MS/MS method for 26 hydroxylated polyunsaturated fatty acids as rapid targeted metabolomics approach for the LOX, CYP, and autoxidation pathways of the arachidonic acid cascade. *Chromatographia* **2015,** *78* (5), 415-428.